Pergamon

0731-7085(94)00093-X

Journal of Pharmaceutical & Biomedical Analysis, Vol. 12, No. 11, pp. 1425–1441, 1994

0731-7085/94 $7.00 + 0.00

Mouse hepatic metabolites of ketoconazole: isolation and structure elucidation

L.W. WHITEHOUSE,* A. MENZIES, B. DAWSON, T.D. CYR, A.W. BY, D.B. BLACK and J. ZAMECNIK

Bureau of Drug Research, Banting Research Centre, Health Protection Branch, Ottawa K1A 0L2, Canada

Abstract: Oxidation, cleavage and degradation of the imidazole and piperazine rings, O-dealkylation, and aromatic hydroxylation are the reported pathways of ketoconazole (KC) metabolism. Metabolites were examined in hepatic extracts from male Swiss Webster mice treated with KC (350 mg kg^{-1} po × 7 days) in a 0.25% gum tragacanth suspension at 10 ml kg^{-1}. Livers were collected 24 h after the last dose and stored at −70°C. A mixture of chloroform/methanol extracts of liver homogenates were dried under vacuum and methanol extracts of the residue were chromatographed by a series of preparative and analytical HPLC techniques. Structure assignments were made by NMR and MS/MS techniques. It was demonstrated that KC was biotransformed to a number of products. Nine were isolated and seven identified as exclusive products of the biotransformation of the 1-acetylpiperazine moiety of KC. This substituent was biotransformed to the following: piperazine (de-*N*-acetyl ketoconazole, DAKC), *N*-carbamylpiperazine, *N*-formylpiperazine, 2,3-piperazinedione, 2-formamidoethylamine, ethylenediamine and amine. The ^{1}H-NMR and MS data suggested that the remaining two metabolites were products resulting from the oxidation of the imidazole ring.

Keywords: *Ketoconazole; metabolism; hepatic metabolism; HPLC; NMR; MS/MS; structure elucidation; piperazine derivatives; imidazole derivatives.*

Introduction

Ketoconazole (Fig. 1) is a potent systemic antimycotic used to treat opportunistic infections in AIDS patients [1] as well as the treatment of a wide range of endocrinological and lipid metabolism disorders [2]. Its potent inhibitory effects on oxidative metabolism has also made this compound a useful chemotherapeutic agent for prostate cancer [3, 4]. The metabolism of ketoconazole is complex. Several pathways, purporting to lead to more than 22 metabolites for humans and animals have been reported, with hepatic microsomal enzymes playing the major role in these biotransformation reactions [5, 6]. Oxidation, scission, and degradation of the imidazole and piperazine rings, scission of the dioxolane ring, O-dealkylation, and aromatic hydroxylation were the suggested metabolic pathways involved in its biotransformation. Surprisingly, there has been little published information to support these purported metabolic pathways. Remmel *et al.* [7] attempted to identify ketoconazole metabolites in bile, urine, and faeces samples collected from rats following intravenous administration of ketoconazole (5 mg kg^{-1}). Only traces of glucuronide and sulphate conjugates of ketoconazole were detected and there was no evidence of O-dealkylated metabolites. Two potential products of O-dealkylation at C-23, 1-*N*-acetyl-4-*p*-hydroxyphenyl piperazine and *p*-hydroxyphenyl piperazine were specifically looked for, but not found in any of the samples examined. To the best of our knowledge, our previous publication [8] has been the only report in the open literature describing a specific product, namely, de-*N*-acetyl ketoconazole, of ketoconazole biotransformation.

The objective of this study was to isolate and characterize other biotransformation products of ketoconazole found in mouse liver.

Materials and Methods

Animals and materials

Male Swiss Webster mice weighing 30 ± 1 g purchased from Charles River Laboratories, (Montreal, Canada), were acclimatized to our animal facility for at least 1 week on inert bedding (Beta Chips) with free access to food

* Author to whom correspondence should be addressed.

and water. All animal procedures and manipulations were in accordance with the Canadian Council on Animal Care Guidelines. Mice were treated with a suspension of ketoconazole (350 mg kg^{-1} po × 7 days) in 0.25% Gum Tragacanth at 10 ml kg^{-1}. Twenty-four hours after the last dose the animals were killed and their livers collected on ice and stored at −70°C until used.

Isolation of ketoconazole metabolites

Sample preparation. Tissue was homogenized (Ultra-Turrax, Janke & Kunkel GmbH & Co KG, D7813 Staufen) with 20 volumes of chloroform–methanol (2:1). Protein was removed by centrifugation and 0.1 N KCl (0.2 volumes) was added to the supernatant to effect phase separation. Chloroform extracts were pooled and dried under vacuum. The lipid residue was extracted 3 times with 2.0 ml of methanol and the combined extract subjected to HPLC.

Preparative high pressure liquid chromatography (HPLC). The methanol extracts were initially separated by preparative-gradient HPLC. Samples were injected onto a 21.2 mm × 25 cm preparative PLC-18 column (Supelco, Inc. Bellefonte, PA, USA) and run at a flow rate of 18 ml min^{-1} using a gradient system of methanol (A) and 0.01 M ammonium hydrogen phosphate pH 3.4 (B) both containing 0.1% triethylamine. Separation was performed by running a system of 70% A and 30% B for 2 min followed by a linear gradient to 85% A over 18 min then a ramp to 100% A to wash the column. Peaks monitored at 254 nm were collected and those of interest were pooled, taken to dryness on a rotary evaporator and redissolved in water. The pH was adjusted to 9.0 with dilute ammonium hydroxide and the resulting solution extracted with chloroform. Extracts were dried under nitrogen, redissolved in methanol and rerun on the preparative HPLC system. Individual peaks were again collected, dried, extracted and dissolved in chloroform.

Analytical high pressure liquid chromatography. The chloroform fractions were injected

Table 1
Chromatographic characteristics of ketoconazole and its metabolites isolated from mouse hepatic tissue

Sample no.	Retention time (min)*	Other chromatographic systems			
		Column†	Mobile‡ phase	Retention time	Mass§ (Da)
I (KC)	12.90	1	A	10.21	531.152
		2	F	12.90	
		2	K	3.20	
II (DAKC)	21.60	2	K	8.03	488.140
III (537-6D)	10.97	1	B	12.24	532.157
		2	G	7.50	
IV (537-6B)	12.11	1	A	9.42	517.167
		2	F	6.27	
V (537-6L)	7.68	1	E	12.30	517.117
		2	I	19.18	
VI (537-6E)	9.39	1	B	9.10	491.135
		2	H	7.27	
VII (499-41)	16.62	2	L	13.46	463.154
VIII (537-6G)	9.43	1	C	6.30	420.096
		2	H	5.00	
IX (537-6J)	6.08	1	B	8.23	563.156
		2	I	12.13	
X (537-6I)	7.22	1	D	10.34	565.177

*Samples were separated on a 0.46 × 25 cm 5 μm LC-18 column using a mobile system of methanol with 0.1% triethylamine (TEA)–ammonium hydrogen phosphate, 50 mM, pH 5.4, also containing 0.1% TEA, 70:30 for 2 min followed by a 16 min linear gradient to 80:20 and held.

†Column 1 was a 0.46 × 25 cm 5 μm LiChrosorb column, and column 2 was a 0.8 × 10 cm Silica 5 μm Radial Pak Cartridge.

‡Mobile phases were methylene dichloride–methanol–ammonium hydroxide with A = 96.7:3.2:0.06; B = 94.0:5.9:0.1; C = 94.4:5.4:0.1; D = 95.4:4.5:0.09; E = 90.7:9.1:0.18; and chloroform–methanol–ammonium hydroxide with F = 95.7:4.3:0.03; G = 91.4:8.6:0.06; H = 92.8:7.1:0.05; I = 92.8:7.1:0.05 for 7 min then 1 min gradient to 71.2:28.5:0.5 and held; J = 95.7:4.3:0.03 for 8 min then 1 min gradient to 75.6:24.2:0.17; K = 88.3:11.0:0.7; and L = 90.3:9.0:0.7. All flow rates were at 1 ml min^{-1}.

§Deviation from calculated mass was always less than 26 mDa.

onto a 5 μm Si radial-pak column (Waters, Millford, MA) and run at 1 ml min^{-1} in a chloroform, methanol, ammonium hydroxide system (see Table 1 for column and solvent ratios used). Fractions collected from this system were dried under nitrogen and re-injected onto a 25 cm analytical 5 μm LiChrosorb column (Brownlee Labs) run at 1 ml min^{-1} with methylene chloride, methanol, ammonium hydroxide (see Table 1 for column and solvent ratios used).

Metabolite VII, the product resulting from the metabolism of the piperazine moiety to the ethylenediamine substituent, was initially isolated from liver extracts that had been dried under nitrogen and redissolved in mobile phase (methanol–ammonium hydrogen phosphate (50 mM) (80:20), pH 3.2, containing 0.1% triethylamine). Samples were chromatographed on a 10 cm Whatman Partisil 5 ODS-3 analytical column at 1 ml min^{-1}. Material collected was dried under nitrogen and dissolved in chloroform and rechromatographed on a Si Radial-Pak column with chloroform–methanol–ammonium hydroxide as described in Table 1, HPLC column 2 and mobile phase L.

Spectral analysis

Nuclear magnetic resonance (NMR). Proton Magnetic resonance spectra (400.13 MHz) were run on a Bruker AM 400 spectrometer at 300K in deuterated methylene chloride (CD_2Cl_2). Resonances spectra of metabolites were compared with those of ketoconazole to determine the presence or absence of component parts of the drug. The ketoconazole spectra will be described in detail using the structure numbering shown in Fig. 1. Subsequent discussion of the spectra of metabolites will simply be related to the parent compound and its numbering. The ^{1}H-NMR spectra of the parent drug and its deacetylated analogue, using deuterochloroform as the solvent, have been previously reported [8, 9]. In this study, deuterated methylene chloride (CD_2Cl_2) was used to avoid the interference of the $CHCl_3$ signal with the resonance for the proton on the 5 position of the dichlorophenyl ring and potentially with a proton on the imidazole ring for some metabolites. This solvent change resulted in some minor chemical shift differences (>0.1 ppm) as well as the broadening of the imidazole resonances, which will be discussed. The assignments of the ^{1}H-NMR resonances for ketoconazole extracted from mouse liver, Fig. 2(c), were as follows: dichlorophenyl ring-doublet at 7.59 ppm with an ortho coupling of 8.5 Hz (H6), a doublet at 7.49 ppm with a meta coupling of 2.1 Hz (H3) and a doublet of doublets at 7.28 ppm with both ortho and meta couplings (H5); the CH2 (H8) appeared as an AB quartet at 4.47 ppm, the imidazole proton resonances appeared as broad singlets at 7.47, 6.97 and 6.92 ppm (H10, H12 and H13), respectively; the H16 protons gave rise to doublets of doublets at 3.88 and 3.74 ppm, the H15 proton signal was a multiplet centred at 4.35 ppm; the H18 proton resonances appeared as doublets of doublets at 3.7 and 3.37 ppm. The para substituted phenyl ring gave rise to a AA'BB' spin system at 6.89 and 6.77 ppm (H22, H24 and H21, H25, respectively), the piperazine protons H27 and H31 appeared as an overlapping pair of doublets of doublets (4 protons) centred at 3.03 ppm. The H28 and H30 protons also appeared as overlapping pairs of doublets of doublets at 3.59 and about 3.7 ppm (4 protons) and the N-acetyl methyl group H33 appeared as a three proton singlet at 2.08 ppm (data not shown).

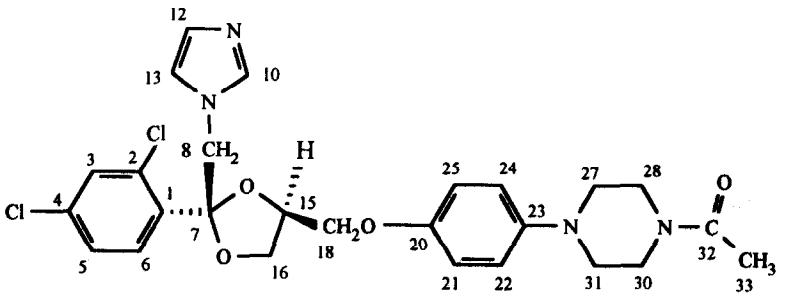

Figure 1
Ketoconazole with adopted structure numbering.

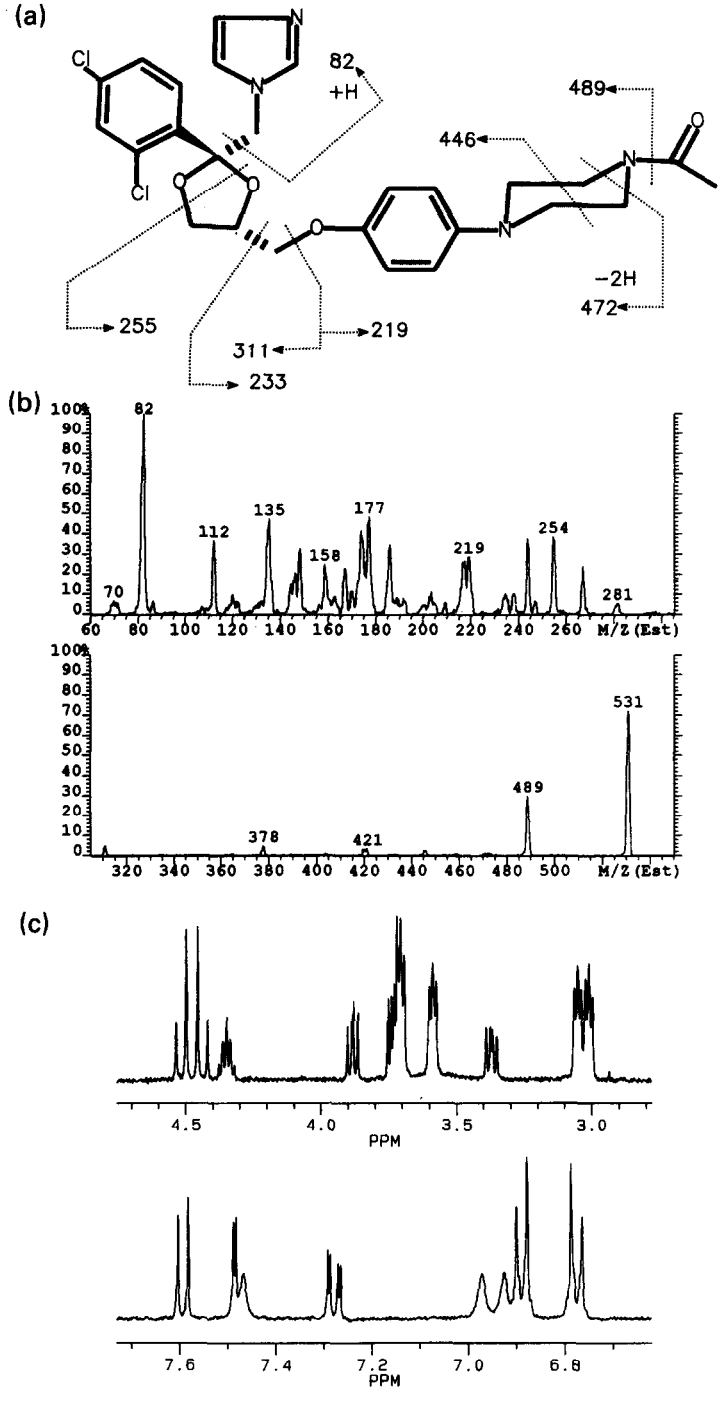

Figure 2
Top (a): ketoconazole structure and MS/MS fragmentation pattern. Middle (b): MS/MS spectrum. Bottom (c): NMR spectrum.

During the course of this study, it was found that the appearance of the signals from the protons close to nitrogen atoms (i.e. those close to the imidazole and piperazine rings) varied in chemical shift and peak widths. This could be explained by either multiple conformers of the analyte, interconverting in the intermediate exchange regime or by the presence of acid in the methylene chloride solution. It was observed that when there was no acid present, the signals for all the protons in these molecules were sharp (i.e. narrow linewidths). However, as acid was introduced, the basic nitrogen sites became protonated and the

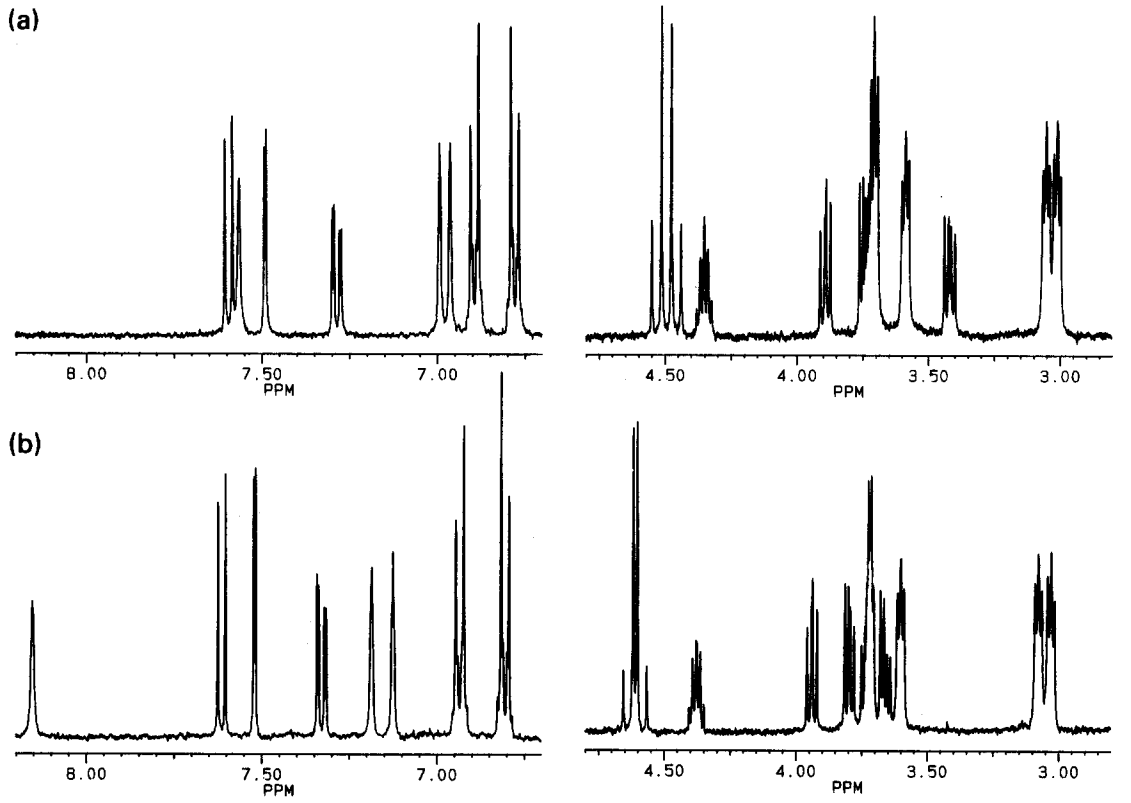

Figure 3
Effect of trace amounts of acid on the NMR of ketoconazole. Top (a): Control. Bottom (b): in presence of acid.

proximate proton signals broadened and shifted to lower field. This is illustrated in Fig. 3: the spectrum of ketoconazole alone and in the presence of acid shows that protonation mainly occurred at N-9 in the imidazole ring as evidenced by changes in the chemical shifts of the protons on carbons 8, 10, 12, 13 and 18. For the metabolites, protonation occurred on the imidazole ring nitrogen and/or on the nitrogens arising from the piperazine ring, depending on the presence or absence of a piperazine carbonyl group affecting the basicity of that ring.

Since many of the metabolites studied were available in such small amounts (low microgram levels), the trace of acid usually found in methylene chloride could have served as the source of acid and caused the protons on the imidazole and piperazine moieties to broaden and shift.

Mass spectrometry (MS). The mass spectra were obtained on a VG AutoSpec Q by liquid secondary ion ionization (LSIMS) using a glycerol matrix and a caesium ion gun, or using a direct exposure probe. The LSIMS technique generally yields protonated molecular ions (M + 1) with very little fragmentation. The mass spectral fragmentation patterns for these polar compounds were obtained by the sequence: compound ionization in the MS source compartment, separation by the (MS) electric/magnetic/electric sector (EBE) of the instrument at unit mass resolution, fragmentation in a gas cell (q) and final analysis with the quadrupole (Q). The overall instrument configuration is EBEqQ. The protonated molecular ions were produced by dissolving the samples in ethanol or methylene chloride at a concentration of approximately 0.5 mg ml^{-1} and adding 1 μl of this solution to a small droplet of glycerol on a metal probe tip. The volatile solvent was removed using a gentle stream of helium. The compounds were ionized from the glycerol matrix with caesium ions using the caesium ion gun operated at 35 kV and the source at 8 kV. Each ion selected by the analyser for MS/MS analysis was defined as the parent ion and, in this case, was the protonated molecular ion of the compound of interest. The parent ion in question was transmitted to the collision cell

Table 2
Nomenclature for ketoconazole and its metabolites

I	Ketoconazole	*cis*-1-acetyl-4-[4-[[2-(3,4-dichlorophenyl)-2-(1*H*-imidazol-1-ylmethyl)-1,3-dioxolan-4-yl]methoxy]phenyl]piperazine
II	Deacetyl-ketoconazole	*cis*-4-[4-[[2-(2,4-dichlorophenyl)-2-(1*H*-imidazol-1-ylmethyl)-1,3-dioxolan-4-yl]-methoxy]phenyl]piperazine
III	N-carbamylpiperazine	*cis*-1-carbamyl-4-[4-[[2-(2,4-dichlorophenyl)-2-(1*H*-imidazol-1-ylmethyl)-1,3-dioxolan-4yl]methoxyl]phenyl]piperazine
IV	N-formylpiperazine	*cis*-4-[4-[[2-(2,4-dichlorophenyl)-2-(1*H*-imidazol-1-ylmethyl)-1,3-dioxolan-4-yl]-methoxy]phenyl]-1-formyl-piperazine
V	2,3-Piperazinedione	*cis*-4-[4-[[2-(2,4-dichlorophenyl)-2-(1*H*-imidazol-1-ylmethyl)-1,3-dioxolan-4-yl]-methoxy]phenyl]-2,3-piperazinedione
VI	2-Formamidoethylamine	*cis*-4-[4-[2-(2,4-dichlorophenyl)-2-(1*H*-imidazol-1-ylmethyl)-1,3-dioxolan-4-yl]-methoxy]-N-(2-formamidoethyl)-aniline
VII	Ethylenediamine	*cis*-*N*-(2-aminoethyl)-4-[4-[2-(2,4-dichlorophenyl)-2-(1*H*-imidazol-1-ylmethyl)-1,3-dioxolan-4-yl]methoxy]aniline
VIII	Amine	*cis*-4-[4-[2-(2,4-dichlorophenyl)-2-(1*H*-imidazol-1-lmethyl)-1,3-dioxolan-4-yl]-methoxy]aniline
IX		*cis*-1-acetyl-4-[4-[[2-(2,4-dichlorophenyl)-2-(1*H*-4,5-dihydroimidazol-1-ylmethyl)-1,3-dioxolan-4-yl]methoxy]phenyl]-piperazine-4-oxide
X		*cis*-1-acetyl-4-[4-[[2-(2,4-dichlorophenyl)-2-(N-formyl-N-(2-aminoethylene)-amino-methyl)-1,3-dioxolan-4-yl]methoxy]-phenyl]piperazine-4-oxide

and fragmented by collisions with argon at a pressure of 2–4 × 10^{-6} mbar. The collision gas cell was programmed from 20 to 35 eV to maximize the fragmentation information. The ions were then transmitted to the quadropole mass analyser to obtain the daughter ion spectra; that is, all the fragmentation ions from a specified parent ion.

The main fragmentation pathway of the protonated molecular ion of ketoconazole (531 Da), Fig. 2(b), was the loss of the acetyl group as ketene to give a peak at mass *m/z* 489. The piperazine ring also may have been cleaved: with loss of acetamide to give *m/z* 472 or loss of acetylaziridine or acetyl-methylvinyl-amine to give *m/z* 446. The *m/z* 311 ion resulted from C-18 bond scission at the phenoxy group, with proton transfer. The *m/z* 219 ion resulted from cleavage of the phenoxy group, loss of ketene (42 Da) from this fragment gave *m/z* 177 which, in turn, may have lost C_2H_4N (42 Da). The *m/z* 135 ion may also have been formed from cleavage of the phenoxy group, then cleavage of the piperazine ring. The *m/z* 255 ion resulted from the cleavage of the oxetane ring such that one of the oxygens remained on each side of the ring scission. The *m/z* 82 peak was the result of fragmentation at the C7–C8 bond to give the protonated imidazole plus methylene group. The isotope peak with two chlorine-37 atoms was analysed independently to determine the presence or absence of the dichlorophenyl group in a fragment. For example, fragmentation of *m/z* 531 gave: 489, 472, 311, 255, 244, 219, 177, 112 and 82 vs *m/z* 533 which gave: 491, 473, 313, 257, 246, 219, 177, 112 and 82. The fragments containing the dichlorophenyl group were readily recognized by their displacement by 2 Da.

Results and Discussion

Chromatographic separation

A typical LC separation of a chloroform solution of ketoconazole and related material isolated following the final preparative LC separation is presented in Fig. 4. De-N-acetyl ketoconazole (II) was isolated from mouse hepatic tissue and unequivocally identified in a

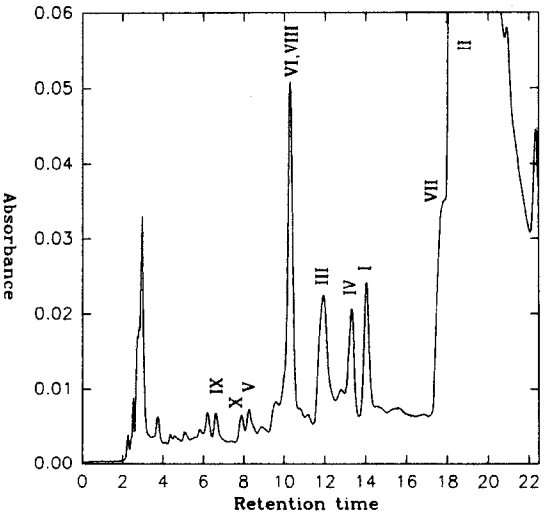

Figure 4
LC separation of ketoconazole and related metabolites. Chloroform extracts of mouse liver previously isolated by preparative LC were separated on a 0.46 × 25 cm 5 μm LC-18 column using the conditions described in Table 1.

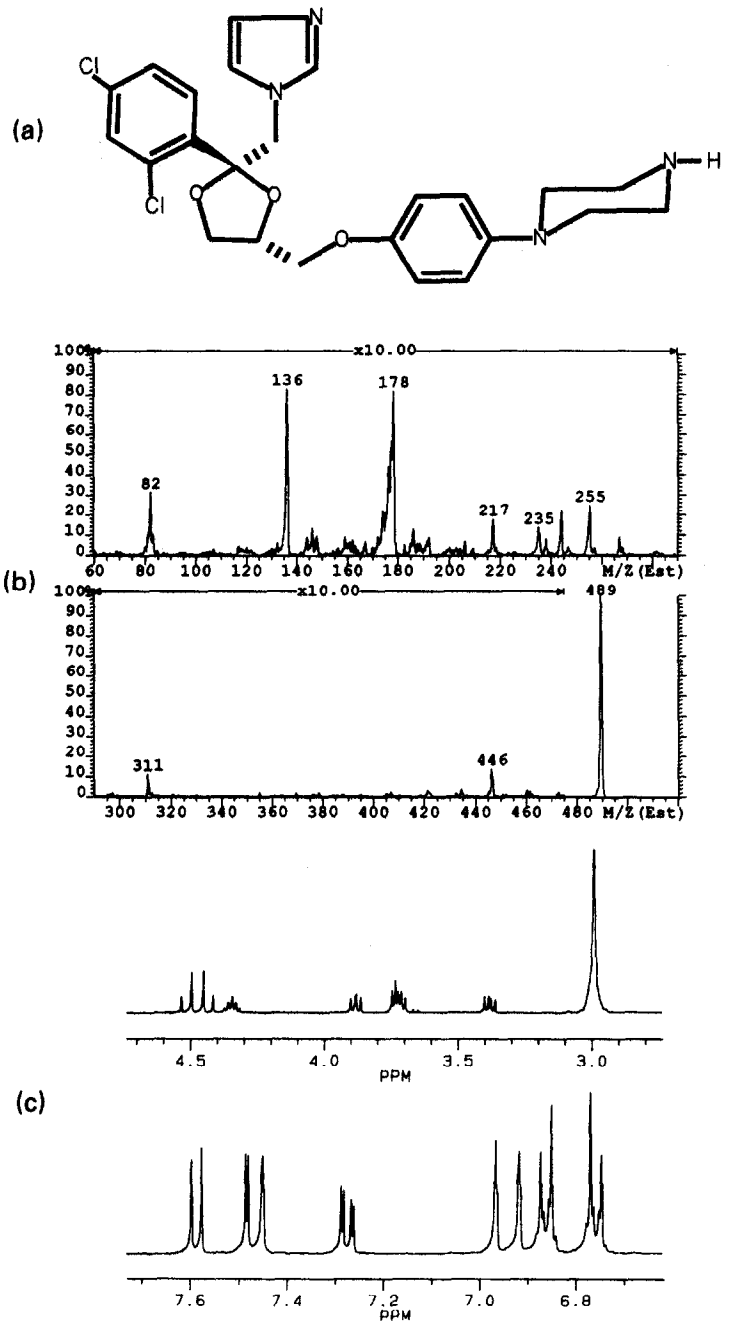

Figure 5
Top (a): Compound II (de-N-acetyl ketoconazole, DAKC) structure and MS/MS fragmentation pattern. Middle (b): MS/MS spectrum. Bottom (c): NMR spectrum.

previous publication [8]. Further examination of mouse hepatic extracts indicated that additional chromatographic peaks could be separated. The chromatographic characteristics of eight additional ketoconazole related products, each of these products run separetely using different columns and mobile phases, are tabulated in Table 1. Ketoconazole and de-N-acetyl ketoconazaole are included for comparison (see Table 2).

Compound II (de-N-acetyl ketoconazole) was identified in the previous publication [8] as the major metabolite detected in mouse hepatic extracts. The NMR spectrum showed the loss of the acetyl methyl group and the presence of all the ring systems (Fig. 5c). In this case all of the piperazine protons coincidentally appeared as a broad single peak. The mass spectrum, Fig. 5(b), (MS/MS of 489 peak) showed no loss of 42 Da (ketene) and

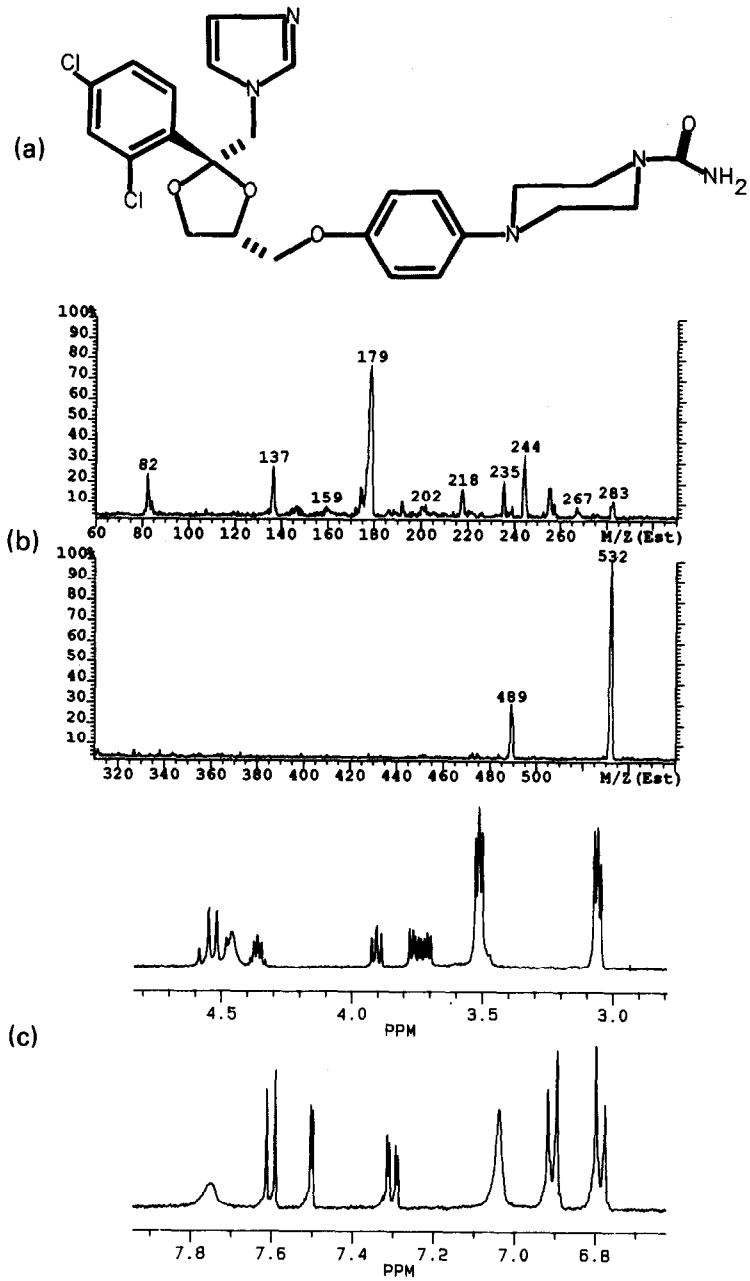

Figure 6
Top (a): Compound III structure and MS/MS fragmentation pattern. Middle (b): MS/MS spectrum. Bottom (c): NMR spectrum.

ions at *m/z*: 446, 255 and 244 due to the ring systems as well as the *m/z* 82 ion due to the imidazole group were noted in the spectra. Ions at *m/z* 178 and 136 represented cleavage of the phenoxy group with subsequent loss of C_2H_4N.

Compound III contained a urea type functional group (Fig. 6a). This structure was confirmed by synthesis from the reaction of de-N-acetyl ketoconazole with potassium isocyanate under acidic conditions as previously described [10]. The ^{1}H-NMR spectrum, Fig. 6(c), indicated the absence of the acetyl methyl group and the presence of all the ring systems of the parent drug, with the addition of a broad singlet at 4.46 ppm due to the NH_2. The mass spectrum, Fig. 6(b), of the protonated molecular ion (*m/z* 532) indicated the loss of 43 Da (O=C=NH)) to give *m/z* 489; the ions: 255, 244, 235, 218, 179 and 136 indicated the presence of the ring systems. The imidazole group (*m/z* 82) and loss of 43 Da (O=C=NH)

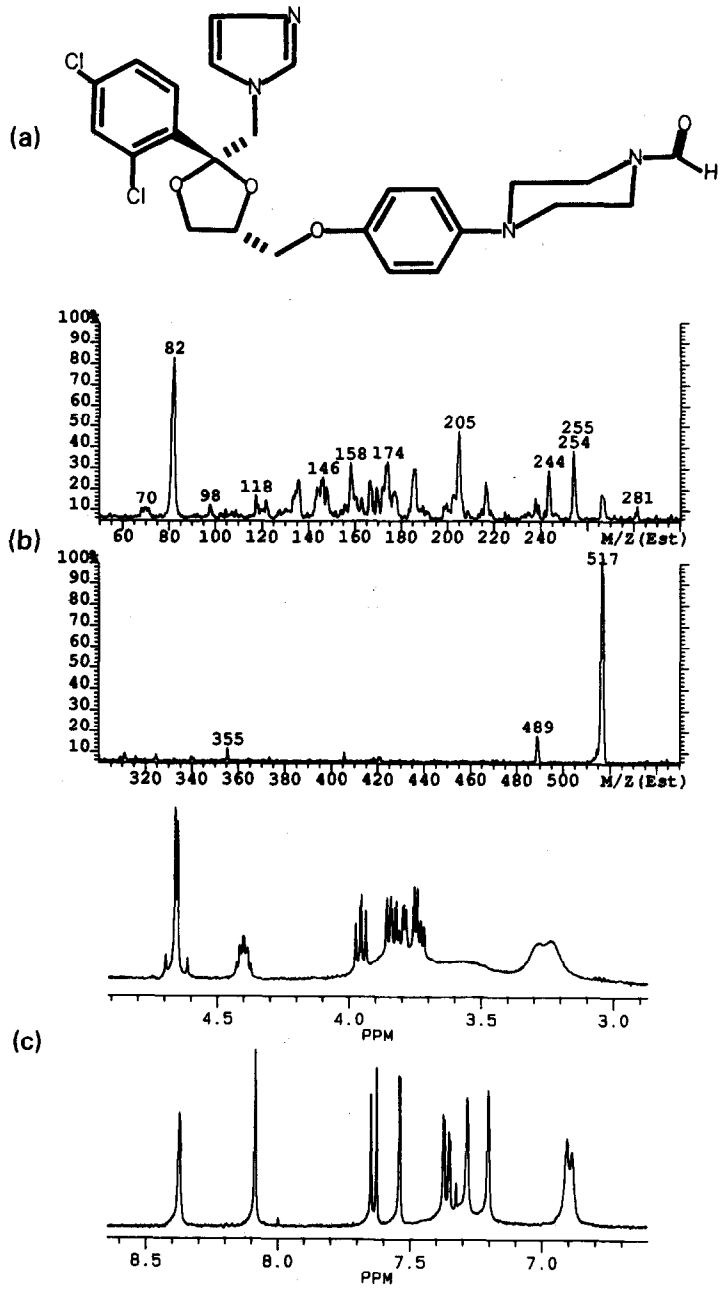

Figure 7
Top (a): Compound IV structure and MS/MS fragmentation pattern. Middle (b): MS/MS spectrum. Bottom (c): NMR spectrum.

and 42 Da (C_2H_4N) to give ions at *m/z* 179 and 137, respectively, were detected.

The ^{1}H-NMR spectrum of compound IV showed an amide proton signal at 8.08 ppm and the presence of all ring systems (Fig. 7c). The resonances for the protons near the piperazine ring nitrogens (on carbons 21–31) were shifted and broadened substantially. The imidazole peaks were shifted to lower field, indicating protonation of this ring as well. The mass spectrum, Fig. 7(b), of the protonated molecular ion (*m/z* 517) showed loss of 28 Da (CO) to give *m/z* 489 and the ring systems *m/z*: 255 and 244 as well as the imidazole ring *m/z* 82. Other diagnostic fragments included: cleavage of the phenoxy ring to *m/z* 205 with further fragmentation (-CO, 28 Da then -C_2H_4N, 42 Da) to ions at *m/z* 177 and 135. This structure, Fig. 7(a), was confirmed by synthesis from the reaction of de-*N*-acetylketo-

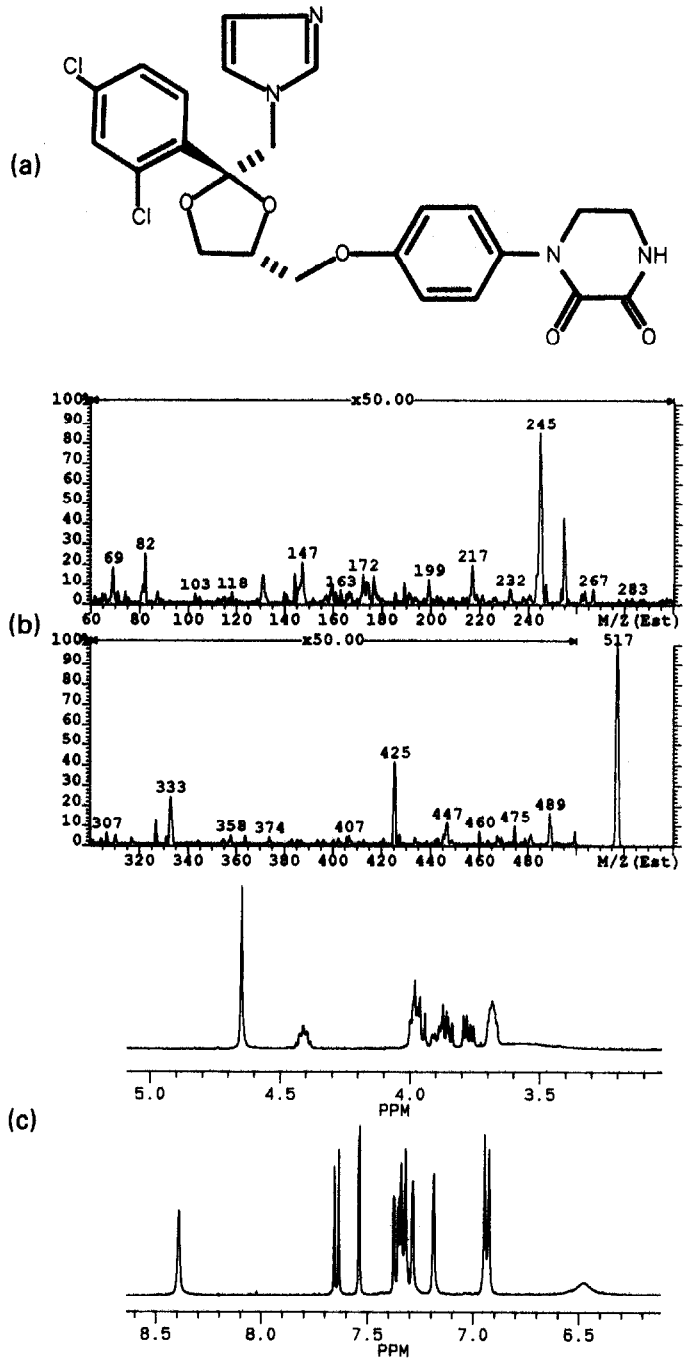

Figure 8
Top (a): Compound V structure and MS/MS fragmentation pattern. Middle (b): MS/MS spectrum. Bottom (c): NMR spectrum.

conazole with formic acid as previously described [11].

The ^{1}H-NMR spectrum of compound V exhibited shifted but sharp resonances for protons on or near the imidazole ring (Fig. 8c). The C8 protons appeared as a singlet at 4.65 ppm. The para substituted phenyl groups protons, H22 and H24, were shifted by 0.44 ppm, but remained sharp. The "piperazine ring" showed four coupled protons overlapped with the signals from those on C16 and C18 in the region 3.1–4.1 ppm. The mass spectrum, Fig. 8(b), of the protonated molecular ion (*m/z* 517) showed an intact oxetane ring (*m/z* 255,

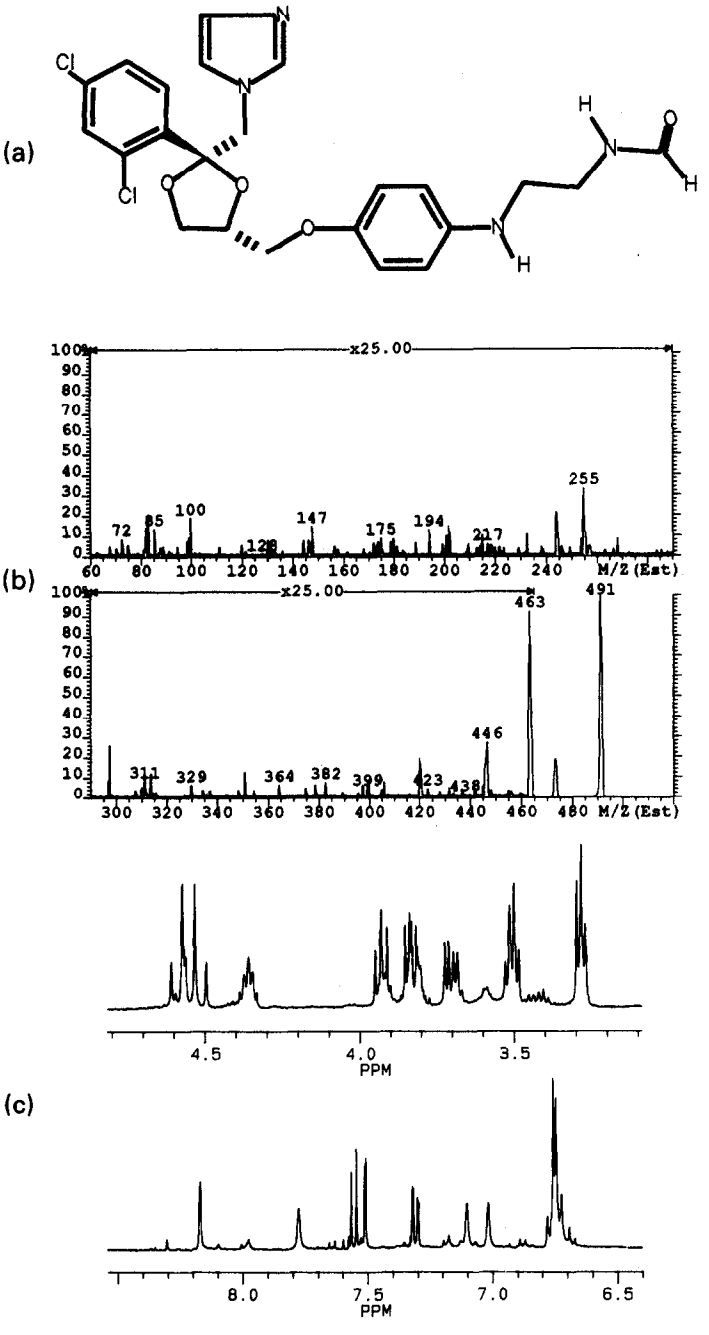

Figure 9
Top (a): Compound VI structure and MS/MS fragmentation pattern. Middle (b): MS/MS spectrum. Bottom (c): NMR spectrum.

244) and the imidazole group (*m/z* 82). The *m/z* 489 and 460 ions resulted from loss of CO (28 Da) and of C_2H_3NO (57 Da), respectively. This data suggested that the piperazine moiety was oxidized to 2,3-piperazinedione, Fig. 8(a).

The ^{1}H-NMR spectrum of compound VI showed the presence of all the ring protons, except the piperazine ring, plus one proton at 8.17 ppm ascribed to the amido proton and two two-proton multiplets, centred at 3.5 and 3.28 ppm, ascribed to the ethylenediamine moiety (Fig. 9c). The protons on the para substituted phenyl ring were more equivalent than in the parent compound, hence their resonances appeared as a tighter multiplet, centred at 6.75 ppm. There were also a number of minor peaks in both the aromatic and aliphatic regions indicating the presence of unidentified, but

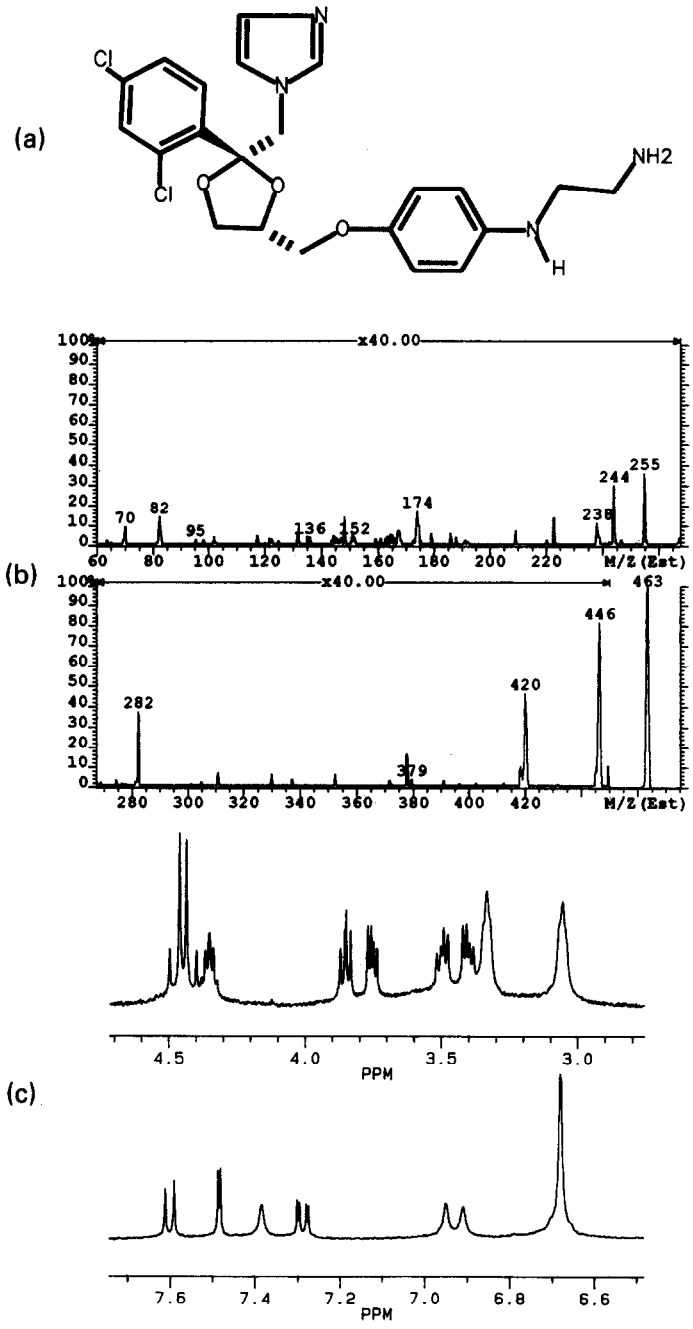

Figure 10
Top (a): Compound VII structure and MS/MS fragmentation pattern. Middle (b): MS/MS spectrum. Bottom (c): NMR spectrum.

probably related, compound(s) at a concentration of approximately 10% relative to the main component. The mass spectrum, Fig. 9(b), of the protonated molecular ion (*m/z* 491) showed a loss of: 18 Da (-H_2O), 28 Da (-CO) and 44 Da (CH(=O)NH), as well as the ring fragments *m/z*: 255, 244 and the imidazole ring *m/z* 82. These spectra are consistent with the ring opened structure shown in Fig. 9(a).

The ^{1}H-NMR spectrum of compound VII showed the presence of all the rings, except the piperazine ring (Fig. 10c). The four protons on the para-substituted phenyl group gave rise to a broad single (6.68 ppm) and the ethylenediamine methylene protons resonated at 3.05 and 3.33 ppm. The mass spectrum of the protonated molecular ion (*m/z* 463, Fig. 10b) showed a loss of 17 Da (NH_3), 43 Da

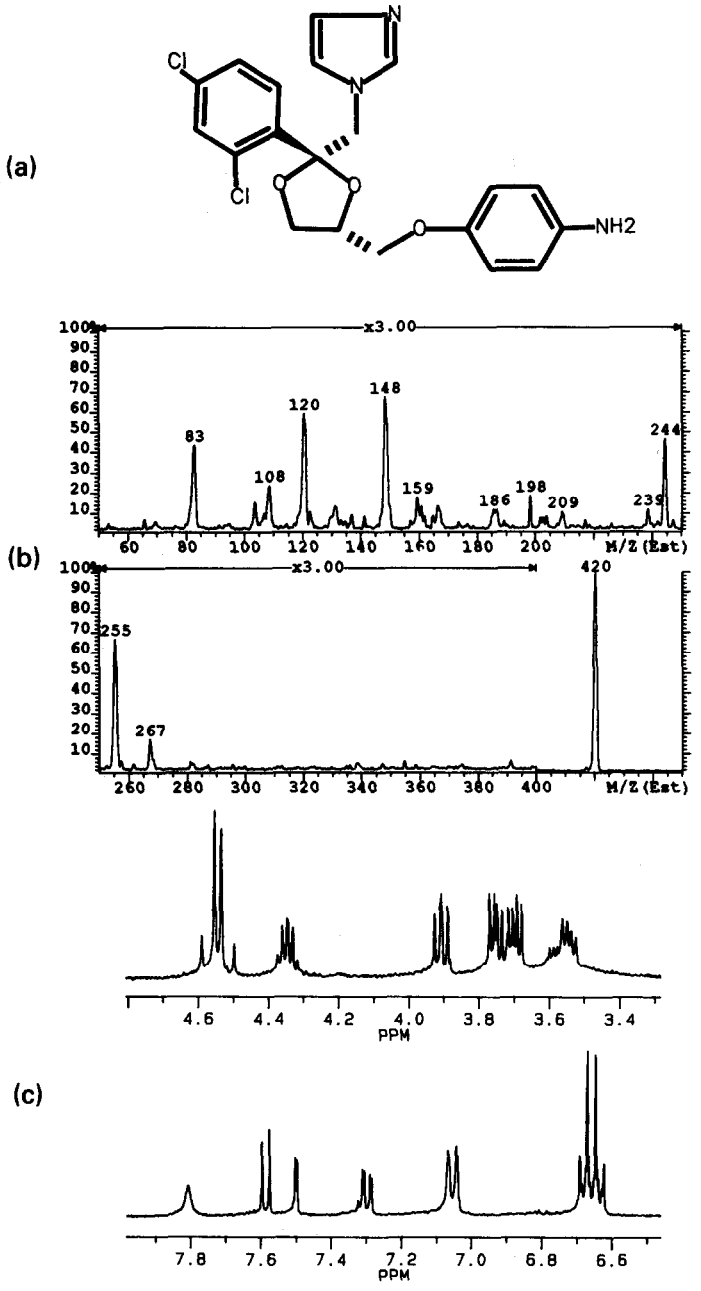

Figure 11
Top (a): Compound VIII structure and MS/MS fragmentation pattern. Middle (b): MS/MS spectrum. Bottom (c): NMR spectrum.

(CH_2=CH-NH_2), presence of the oxetane ring system (*m/z* 255, 244) and the imidazole ring (*m/z* 82). The evidence is consistent with the ethylenediamine structure shown in Fig. 10(a).

The ^{1}H-NMR spectrum of compound VIII showed resonances for all the ring protons except for piperazine (Fig. 11c). The only other proton resonance observed in this spectrum was the addition of a broad NH_2 peak at 3.55 ppm, which was overlapped with a multiplet for one of the C18 protons. The mass spectrum of the protonated molecular ion (*m/z* 420, Fig. 11b) showed the oxetane ring system (*m/z* 255, 244), the imidazole ring (*m/z* 82) and cleavage of the phenoxy group (*m/z* 108). These data are consistent with the degradation of the amine, Fig. 11(a).

The ^{1}H-NMR spectrum of compound IX showed the presence of the dichlorophenyl

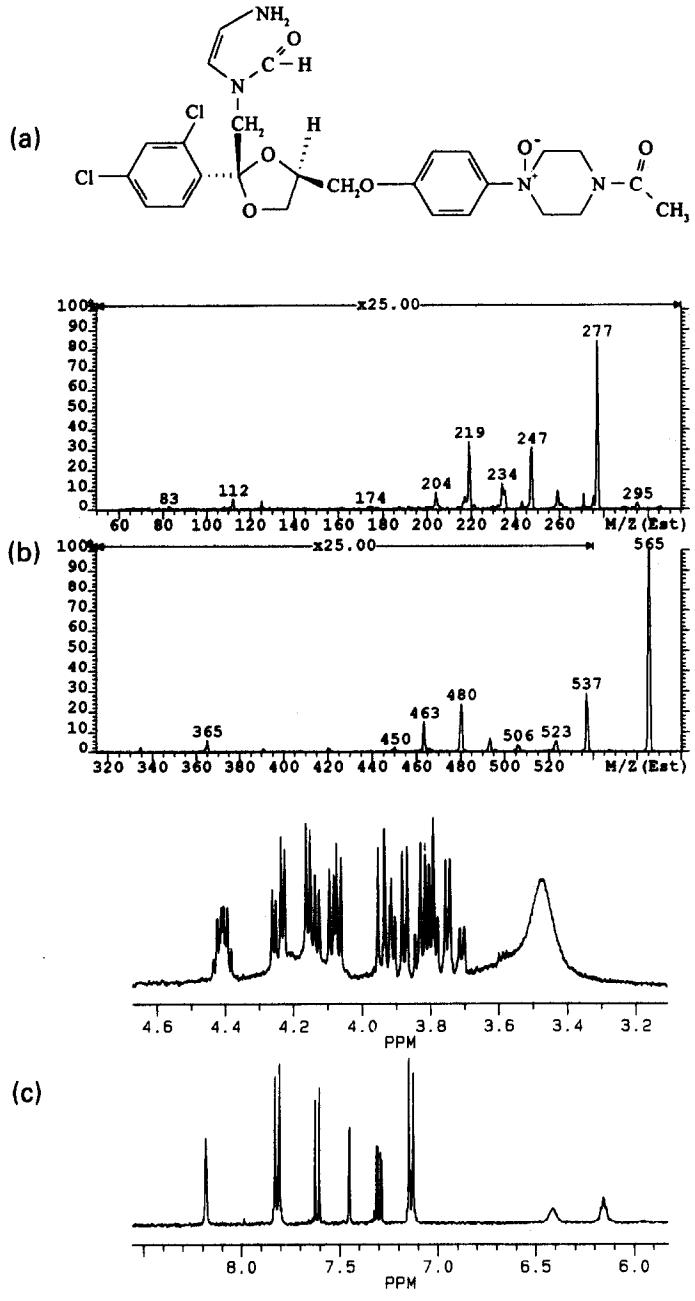

Figure 12
Top (a): Compound IX structure and MS/MS fragmentation pattern. Middle (b): MS/MS spectrum. Bottom (c): NMR spectrum.

ring, the oxetane ring and the para substituted phenyl ring (Fig. 12b). The resonances for one pair of protons of the para substituted phenyl ring were shifted downfield by about 0.9 ppm while those for the other pair were shifted less than 0.3 ppm, with respect to those for ketoconazole. This would be consistent with a strongly electron withdrawing group near C-23. A broad one-proton singlet appearing at 7.34 ppm was ascribed to the "imidazole" ring. There are no other aromatic resonances present which could be attributed to an imidazole type ring system. Integration of the proton signals in the region 3.0–5.0 ppm indicated resonances for about 26 protons. The mass spectrum of the protonated molecular ion (*m/z* 563, Fig. 12a) was an increase of 32 Da over the parent ketoconazole; this suggested the addition of two oxygen atoms or one sulphur atom. The fragmentation pattern

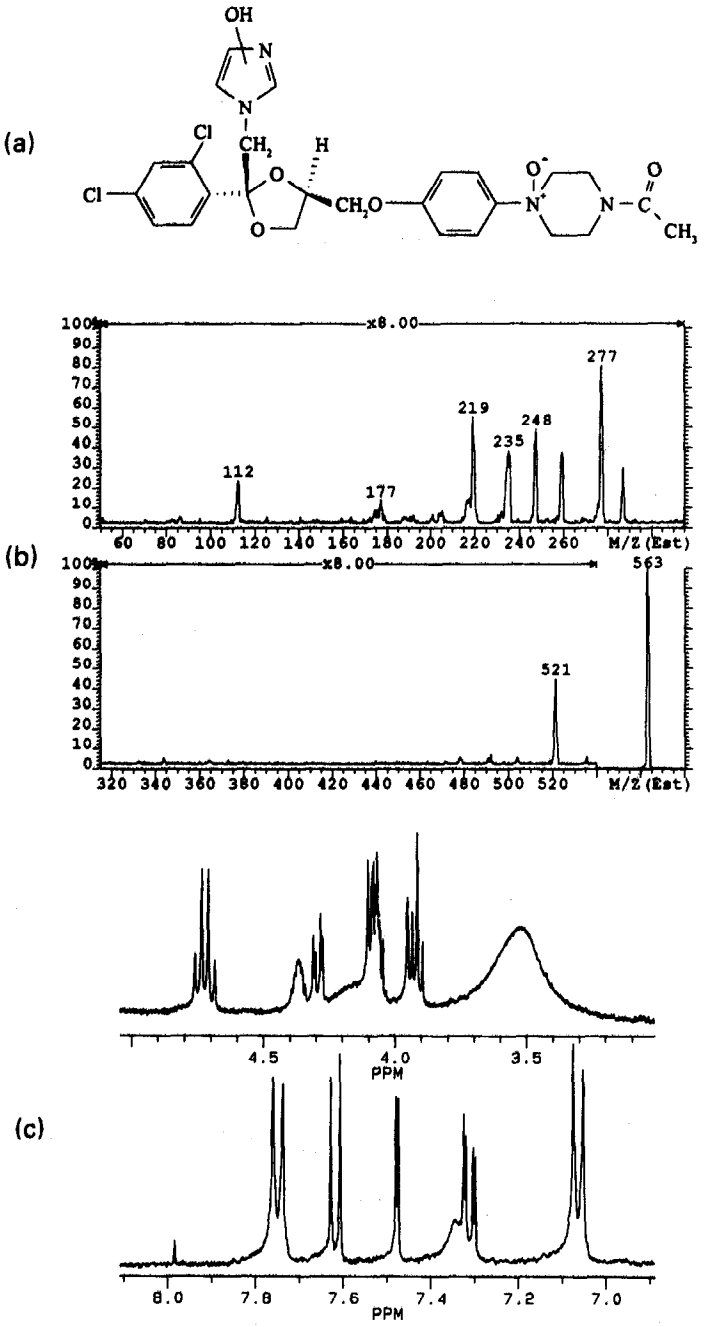

Figure 13
Top (a): Compound X structure and MS/MS fragmentation pattern. Middle (b): MS/MS spectrum. Bottom (c): NMR spectrum.

showed a loss of 42 Da (CH_2CO), but *m/z*: 255, 244 or 82 ions were absent, indicating an altered imidazole group. The cleavage of the phenoxy group, assuming a tertiary amine oxide on the piperazone ring gave a *m/z* 235 peak, which in turn could fragment to give 219, then a 177 peak.

The ^{1}H-NMR spectrum of compound X showed a singlet at 8.18 ppm ascribed to an amide proton, broadened signals for one proton each at 6.15 and 6.41 ppm, and evidence for the presence of the oxetane, dichlorophenyl and the para-substituted phenyl rings (Fig. 13b). The resonances from one pair

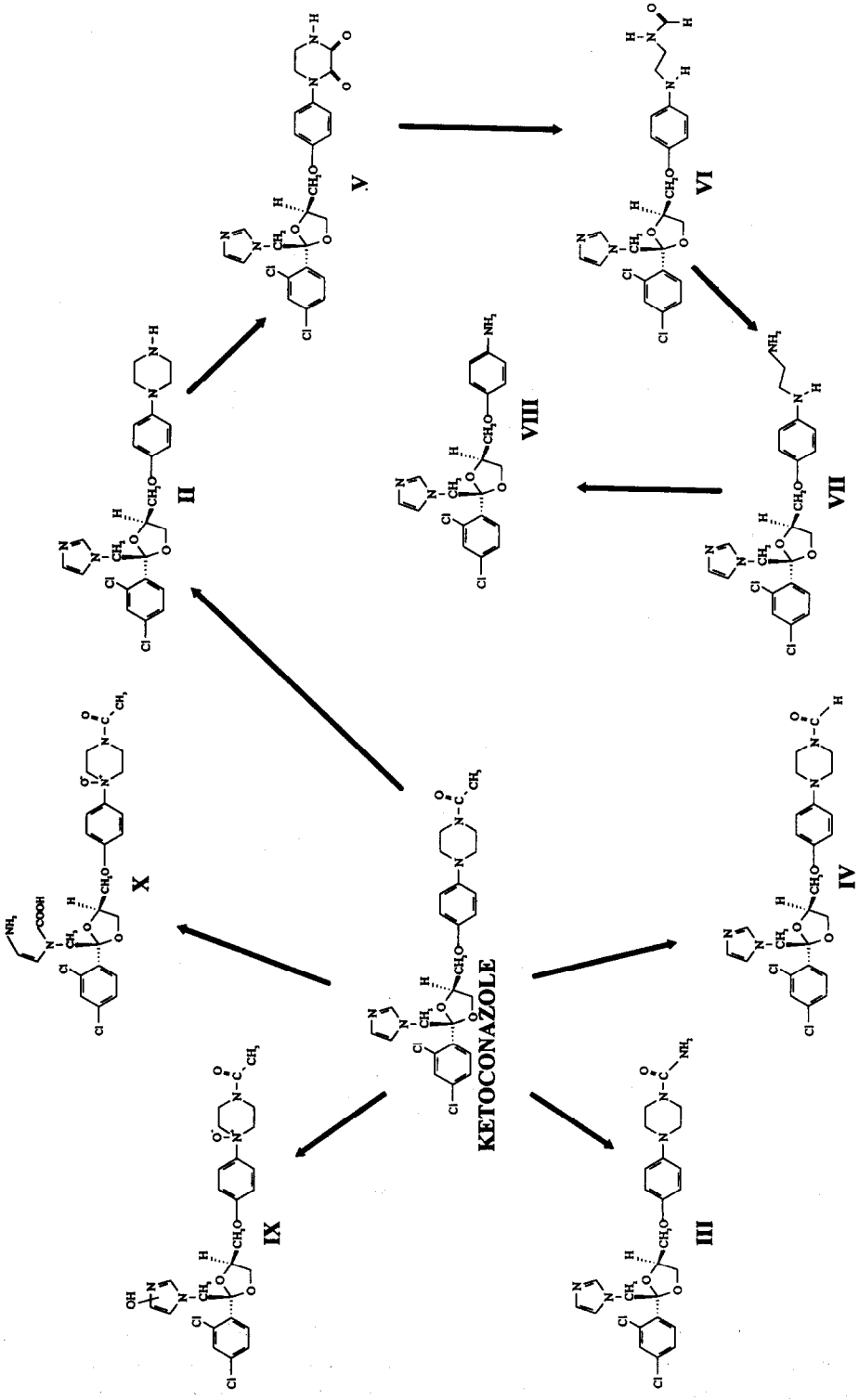

Figure 14
Metabolic scheme for ketoconazole metabolism by Swiss Webster mice.

of protons of the para substituted ring was shifted by more than 0.9 ppm downfield (7.82 ppm), while the other pair was shifted about 0.4 ppm (to 7.13 ppm) with respect to the corresponding ketoconazole resonances. The C8 protons were no longer at 4.5 ppm; they appeared to be shifted to 3.7–3.9 ppm, possibly as a result of the loss of the aromaticity in the imidazole ring. Integration of the region 3.0–4.5 ppm indicated signals for about 20 protons, including six in a broad hump centred at 3.48 ppm. The mass spectrum of the protonated molecular ion (*m/z* 565, Fig. 13a) showed the loss of 28 (CO), a loss of 42 (CH_2CO), 59 ($CH_3C(O)NH_2$) and 72 Da ($CH_3C(O)N(H)CH_2$) but the absence of *m/z*: 255, 244 or 82 peaks indicated changes to the usual ring systems.

Compounds IX and X have similar structures since the mass spectra of both had ions at *m/z*: 277, 259, 235, 219 and 112 and both molecular ions exhibited losses of 42, 59, 72 and 85 Da. The difference between the two compounds appears to be the position of imidazole ring oxidation. The presence in IX of only one proton which could be ascribed as having arisen from this ring, indicated that oxidation to a carbonyl group occurred at the C-12 or C-13, leaving the proton on C-10 in the aromatic region. The mass spectra of compound IX showed the addition of two oxygen atoms with no change in the number of double bond equivalents. The first major fragment peak resulted from a loss of 42 Da which may have been due to ketene from the acetyl side chain of the oxygenated-imidazole ring. In metabolite X, the presence of an amide resonance and two one-proton resonances around 6.0–6.5 ppm indicated oxidation at C-10. The large chemical shift differences between IX and X compared to ketoconazole for protons on C-21–C-25 could have arisen from oxidation at N-26. The mass spectrum for compound X showed a large peak due to the loss of 28 Da (CO) as well as several fragments (463, 480 and 494) arising from intermediates losing 43 Da ($CHCHNH_2$). Therefore, the structure proposed for X oxidation required oxidation to the 26-*N*-oxide and oxidative ring opening of the imidazole ring to a *N*-formamide, *N*-enamine.

This study demonstrated that in the Swiss Webster mouse the piperazine moiety of ketoconazole was readily metabolized. Ketoconazole was shown to be biotransformed to nine metabolites (Fig. 14), seven of which were exclusively products of the metabolic alteration of the *N*-acetylpiperazone ring; namely, piperazine (DAKC), *N*-carbamylpiperazine, *N*-formylpiperazine, 2,3-piperazinedione, *N*-formylethyldiamine, ethyldiamine and amine. The remaining two metabolites were products resulting from the oxidation of the imidazole ring.

References

[1] C.A. Knupp, C. Brater, J. Relue and R.H. Barbhaiya, *J. Clin. Pharmacol.* **33**, 912–917 (1993).
[2] N. Sonino, *J. Endocrinol. Invest.* **9**, 341–347 (1986).
[3] J. Trachtenberg and A. Pont, *Lancet* **2**, 433–435 (1984).
[4] T.K. Daneshmend and D.W. Warnock, *Clin. Pharmacokinet.* **14**, 13–34 (1988).
[5] E.W. Gascoigne, G.J. Barton, M. Michaels, W. Meuledermans and J. Heykants, *Clin. Res. Rev.* **1**, 177–187 (1981).
[6] A.L. Hume and T.M. Kerkering, *Drug Intelligence and Clin. Pharm.* **17**, 169–174 (1983).
[7] R.P. Remmel, K. Amoh and M.M. Abdel-Monem, *Drug Metab. Dispos.* **15**, 735–739 (1987).
[8] L.W. Whitehouse, A. Menzies, B. Dawson, J. Zamecnik and W.-W. Sy, *J. Pharm. Biomed. Anal.* **8**, 603–606 (1990).
[9] B.A. Dawson, *Can. J. Spectrosc.* **35**, 27–30 (1990).
[10] J. Heeres, L.J.J. Backx and J.H. Mostmans, *Chem. Abst.* **98**, 126107g (1983). U.S.A. Patent 4,358,449. 9 November 1982.
[11] J. Heeres, *Chem. Abst.* **86**, 29811b (1977). Ger. Offen. 2,602,770. 29 July 1976.

[Received for review 22 April 1994; revised manuscript received 1 July 1994]